Science Press

ARTICLE

Effect of Zn^{2+} Co-doping on Scintillation Properties of Ce-doped $Gd_3Ga_3Al_2O_{12}$ Ceramic Powder Prepared by Co-precipitation Method

Qiu Zhihua[1],   Zhang Xianhui[2],   Wang Shuaihua[1],   Wu Shaofan[1],   Lin Yonghong[2]

[1] Collaborative Innovation Center for Optoelectronic Semiconductors and Efficient Devices, Fujian Institute of Research on the Structure of Matter, Chinese Academy of Sciences, Fuzhou 350002, China; [2] University of the Chinese Academy of Sciences, Beijing 100049, China

Abstract: Zinc co-doped Ce:$Gd_3Ga_3Al_2O_{12}$ (Ce:GAGG) ceramic precursors were synthesized by chemical co-precipitation method. Thermogravimetric analysis and differential thermal analysis of the precursor powders were performed. The chemical molecule of precursors was analyzed by FTIR. The phases and morphology of the precursors at different calcination temperatures were studied by XRD and SEM. The results show that precursor powders consist of $GdAlO_3$ and GAGG phases at 883 °C. Precursors completely convert to Ce:GAGG powders at 900 °C. The particles of Ce:GAGG powders calcined at 1200 °C range from 20 nm to 60 nm, and become homogeneous and smooth. The effect of polyethylene glycol (PEG) on the morphology of precursors was investigated. Particle size and size range of Ce:GAGG powders calcined at different temperatures were investigated. The influence of Zn^{2+} content on photoluminescence, radioluminescence, excitation spectra and fluorescent lifetime of Ce:GAGG was analyzed. The emission spectrum of Ce:GAGG co-doped with 0.4 mol% Zn^{2+} has the highest intensity. Zn^{2+} in Ce:GAGG powders has a positive effect on reducing the fluorescence lifetime.

Key words: co-precipitation method; precursors; Ce:GAGG ceramic powder; zinc codoping

Scintillator materials can convert high-energy particles like γ-ray and X-ray photons into pulsed light[1-4] which can be further detected by an optical receiving unit or photo-multiplier tube, and have been widely used in high energy physics, medical imaging, industrial inspection, space physics, security screen and geological exploring[5,6]. In the past few years, because of good optical transparency, easy doping by rare-earth elements, and promising candidate hosts in scintillator applications, great effort has been made to develop more efficient and fast scintillators based on cerium-doped aluminate garnets. The Ce-doped $Lu_3Al_5O_{12}$ (Ce:LuAG) has become a prospective scintillator for high light yield, fast decay time, high transmittance and its satisfactory stopping power[7-9]. Considering the higher cost of lutetium in industrial applications, researchers have attempted to replace lutetium by some guidance methods for lowering cost and even achieving better properties. Re-

cently, the methods of band gap engineering have been developed for searching multi-component garnet compounds and it has been found that Ce-doped $Gd_3Ga_3Al_2O_{12}$ (Ce:GAGG) crystals show good scintillation properties. Except for high density (6.63 g·cm^{-3}), Ce:GAGG has many other advantages such as good energy resolution, stable chemical stability and high light yield (>50000 photos/MeV)[10,11]. In previous research, Chen et al[12] reported the preparation of transparent Ce:GAGG ceramics sintered at 1650 °C in flowing oxygen gas, which show an excellent microstructure and a good transmittance of 60% at 560 nm. Kanai[13] prepared Ce:GAGG ceramics by the hot-pressing method, which show a higher light yield of 55 000 photos/MeV and a slower decay time (~90 ns). As we know, the preparation of ceramic powders and the process of ceramic sintering are important for ceramic production. It is a vital key to prepare ceramic nano-powders before sintering scin-

tillation ceramics. In general, the quality including size, morphology and distribution of powders has a obvious effect on properties of scintillation ceramics. In particular, the powders with small size, spherical particles and homogeneous distribution can promote the ceramic sintering. Therefore, more and more attention has been paid to improve the properties of ceramic powders.

In addition, it has been found that co-doping is effective in changing the scintillation properties of garnet materials. Besides, researchers paid more attention to optimizing the composition of different cation concentrations. Chewpraditkul[14] reported that the replacement of octahedrally-coordinated Al^{3+} with Ga^{3+} results in a blue-shift of the Ce^{3+} 5d-4f luminescence band in co-doped Ce:GYGAG single crystal. Chen et al[15] reported transparent Ce^{3+}-doped $Gd_3(Al_{1-x}Ga_x)_5O_{12}$ ceramics, and a blue shift was observed in the $5d_1$ excitation band and 5d→4f of Ce^{3+}. Koschan[16] reported the effect of Ca^{2+} co-doping in cerium-doped GSO and results show that samples co-doped with Ca^{2+} exhibit a notable reduction in charge carrier trapping and decay time. Lin[17] reported that nano-powder co-doping transition metal ions (Zn^{2+}, Mn^{2+}) show an outstanding luminescent intensity. Therefore, luminescent materials co-doped with transition metal ions (Mg^{2+}, Zn^{2+}, Mn^{2+}, Co^{2+}) can also exhibit a high photoluminescence quantum yield, good photostability, low self-absorption and long fluorescent lifetime. The main reason for properties improvement may be attributed to the modification of electronic excitation transfer process accomplished through band gap engineering, and the tailoring of the activation level energy within the gap, achieved by a variation of the garnet composition[18,19]. Moreover, Ce-activated garnet materials co-doped with divalent ions (Mg^{2+}, Zn^{2+}, Mn^{2+}, Co^{2+}) cause the oxidation of a fraction of Ce^{3+} into Ce^{4+} ions[20]. Two kinds of valence state of Ce (Ce^{3+} and Ce^{4+}) are involved in the scintillation process with different kinetics, which leads to an improvement in time resolution[21-23]. Therefore, garnet materials modified by co-doping divalent ions can be an alternative way to improve optical properties of scintillation materials. To the best of our knowledge, little work has been reported in effect of Zn^{2+} co-doping in Ce-doped GAGG ceramics.

In this work, chemical co-precipitation method was used to fabricate Ce:GAGG ceramic nano-powders with various co-doped contents of Zn^{2+}, and effect of different calcination temperatures on precursors was analyzed. The effect of various Zn^{2+} co-doping contents on photoluminescence, radioluminescence, excitation spectra, fluorescent lifetime and diffused reflectance spectrum of Ce:GAGG ceramic nano-powders was also investigated.

1 Experiment

1.1 Materials

All reagents were of analytical grade, and used directly without further purification. Nitrites of $Gd(NO_3)_3\cdot6H_2O$, $Al(NO_3)_3\cdot9H_2O$, $Ga(NO_3)_3\cdot6H_2O$, $Ce(NO_3)_3\cdot6H_2O$ and $Zn(NO_3)_2\cdot6H_2O$ were purchased from Sinopharm Chemical Reagent Co., Ltd. Ammonium hydroxide ($NH_3\cdot6H_2O$), ammonium bicarbonate (NH_4HCO_3), and polyethylene glycol (PEG) were derived from Shanghai Macklin Biochemical Co., Ltd. Distilled water was fully used throughout the preparation process.

1.2 Reaction

The ceramic powders were synthesized by chemical co-precipitation method. Solution of 10 mL $NH_3\cdot H_2O$ (0.1 mol/L) and 12 g NH_4HCO_3 sealed in 200 mL deionized water were used as mixed precipitants with or without 1 wt% PEG. A mixture of $Gd(NO_3)_3\cdot6H_2O$ (15 mmol), $Al(NO_3)_3\cdot9H_2O$ (10 mmol), $Ga(NO_3)_3\cdot6H_2O$ (15 mmol), $Ce(NO_3)_3\cdot6H_2O$ (0.05 mmol) and $Zn(NO_3)_2\cdot6H_2O$ (0~0.05 mmol) was sealed in 200 mL deionized water. Then the mixed solution was slowly dropped into the mixed precipitants under strong magnetic stirring. After precipitation process, the suspension was stirred consistently for half an hour. Then, the suspension was filtered and washed with distilled water and then dried. After above-mentioned preparation, the precursors with or without PEG were obtained. Subsequently, dried precursors were calcined in air for 2 h at 800, 900, 1000, 1100 and 1200 °C to remove the residuary carbonate, nitrate and hydroxide. Finally, Zn^{2+} co-doped Ce:GAGG ceramic powders were obtained.

1.3 Instrumentation

Thermogravimetric analysis and differential thermal analysis (TG/DTA) of the precursor powders were performed by a TG/DTA analyzer (STA449F3) at a heating rate of 10 °C/min. The precursor and calcined powders at different temperatures were investigated by X-ray diffraction (XRD, Miniflex600). Particle size and morphology of calcined powders were examined by field emission scanning electron microscopy (FESEM, SU8010). Photoluminescence (PL) and radioluminescence (RL) spectra of the powders were tested through a fluorescence spectrophotometer (FLS980) using a Xe-lamp (500 W) source and an X-ray source (Moxtex, Magpro, 60 kV, 200 μA, W-target, 12 W) at room temperature. Diffuse reflectance spectrum of the optimized powder was studied by an ultraviolet spectrophotometer (Lambda950). Fluorescent lifetime was measured by a fluorescence spectrophotometer FLS980 using a Xe-lamp (500 W) source (λ_{ex}=350 nm, λ_{em}=530 nm) at room temperature.

2 Results and Discussion

2.1 Thermal analysis and reflectance spectrum

As shown in Fig.1a, TG/DTA curve of the precursor powders is obtained from room temperature to 950 °C at a heating rate of 10 °C/min. The three endothermic peaks at 119, 221 and 437 °C may be due to the removing of free water and bound water. The exothermic peak at 883 °C is

attributed to the formation of $GdAlO_3$ and $Gd_3Al_3Ga_2O_{12}$ phases, which are confirmed by X-ray diffraction. Mass loss of the precursor powders from room temperature to 950 °C is about 30%. About 25% mass loss rapidly takes place between room temperature and 437 °C. In this interval, the mass loss is assigned to the removing of free water and bound water. The remaining mass loss which occurs between 437 °C and 950 °C is about 5%. The mass loss in this stage can be easily ascribed to the decomposition of carbonates, nitrates and hydroxides.

The diffuse reflectance spectrum of Ce:GAGG powders co-doped with 1.0 mol% Zn^{2+} was obtained with the background of $BaSO_4$ powders, as shown in Fig.1b. The reflectivity above 500 nm is up to the maximum, which indicates that the sample has little absorption in this interval. The decreasing of reflectivity at 400~500 nm is attributed to the absorption wavelength of Ce:GAGG powders.

2.2 FTIR spectra of precursors and X-ray diffraction of calcined powders

Fig.2a shows the FTIR spectrum of precursors. The absorption peak at 580 cm^{-1} is attributed to metallic bond (M-O) stretching vibration. We can also find the absorption peak at 1390 cm^{-1} which is originated from C-O bond stretching vibration. O-H bond stretching vibration at 1637 and 3453 cm^{-1} may arise from water.

The phase of the precursor powders and calcined powders at 800, 900, 1000, 1100 and 1200 °C is shown in Fig.2b. The precursor powders in a form of smooth peak are amorphous. The precursor's composition (Gd, Ga, Ce, Zn) $(OH)_x(CO_3)_y \cdot nH_2O$ is carbonate hydroxide salt which is attributed to the NH_4HCO_3 precipitator. There are two processes including the loss of water and the decomposition of carbonate hydroxide salt below 800 °C. Characteristic peaks of $GdAlO_3$ and GAGG are detected in the powders calcined at 800 and 850 °C. The characteristic peaks of $GdAlO_3$ phase disappear at 900 °C, which indicates that 900 °C is the transition temperature of pure GAGG phase. Pure GAGG phases above 900 °C are attributable to the transformation of $GdAlO_3$ phases. This experimental result coincides with the exothermic peak at about 883 °C of the TG/DTA curve. Besides, refined peak and intensity of GAGG phases are observed as the temperature increases from 900 °C to 1200 °C. This indicates that the crystallites of GAGG powders grow as the temperature increases.

2.3 Effect of PEG on morphology of precursor powders

Morphology of precursor powders with or without 1.0 wt% PEG dried at 200 °C is shown in Fig.3. In comparison with the precursor powders without PEG, the morphology of precursor powders with 1.0 wt% PEG becomes dispersive. Most precursor powders with PEG

Fig.1 TG/DTA curve of Ce:GAGG precursors (a) and diffuse reflectance spectrum of Ce:GAGG co-doped with 1.0 mol% Zn^{2+} (b)
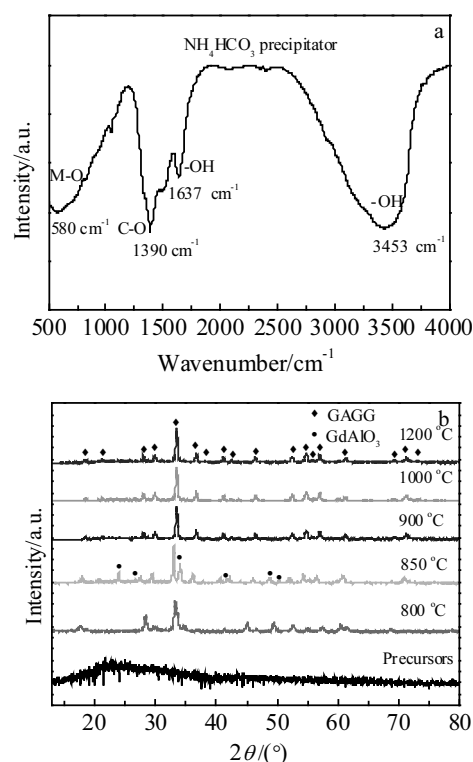
Fig.2 FTIR spectrum of precursors (a) and XRD patterns (b) of Ce:GAGG powders calcined at different temperatures

are in the form of flakes. This indicates that the addition of 1.0 wt% PEG has an obvious effect on morphology and distribution of precursor powders. The main reason for this behavior is that the PEG dissolved in the reaction system can effectively inhibit the agglomeration of precursor powders by adsorbing at the solid-liquid interfaces[24]. The existence of PEG in the reaction system can not only reduce the surface tension to lower adsorbability of precursor powders, but also enhance the steric hindrance effect to reduce the powder force (van der Waals force, Coulomb force and chemical bonding force). Therefore, optimized precursor powders with 1.0 wt% PEG are analyzed further.

The calcination temperature above 900 °C is the optimized interval according to TG/DTA curves and XRD results. Fig.4a~4d show the morphology of Ce:GAGG powders calcined at 900, 1000, 1200 and 1400 °C for 2 h. Powders at 900~1000 °C loosely aggregates primary particles with a size of 20~60 nm, existing in states of lump and granulation. Sintering necks can be hardly found in GAGG powders at 900~1000 °C. When calcined at 1200 °C, powders with a size of 20~60 nm become homogeneous and smooth, and some sintering necks appear. When the calcination temperature increases to 1400 °C, more and more sintering necks appear. At the same time, particles with a size of 110~200 nm become regular and smooth, and grow with the disappearance of grain boundary.
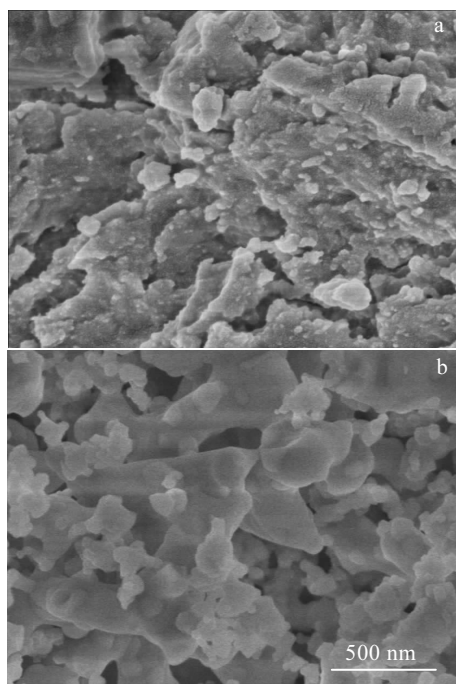
Fig.3   SEM images of Ce:GAGG precursors at 200 °C without PEG (a) and with 1 wt% PEG (b)

2.4   Morphology of GAGG nano-powders

Morphology of calcined Ce:GAGG powders have effects on ceramics sintering, as the powders are under a densification process in ceramics sintering. The particles with small and uniform size, high specific surface area and activity can promote sintering densification of ceramics[25,26]. However, agglomeration happens severely as the particles size decreases, which may result in low bulk density. Therefore, it is important to control the appropriate and uniform size of the particles in the calcination process (Fig.4c). Alternatively, too many necks in particles of Ce:GAGG powders have negative effects on further ceramic sintering. As shown in EDS spectra in Fig.4e and 4f, it can be successfully found that Ce:GAGG powders co-doped with 0.4 mol% Zn^{2+} consist of Gd, Ga, Al, O, Ce and Zn elements. The EDS spectra is consistent with XRD results.

The measured particle size of Ce:GAGG powders calcined at different temperatures is given in Fig.5. The size range of particle calcined below 1200 °C is controlled within a reasonable range from 20 nm to 60 nm, while that of particle calcined at 1400 °C increases from 110 nm to 200 nm, consistent with SEM results. Table 1 reveals statistical results of size range and mean size of Ce:GAGG powders. it can be successfully found that the mean size of Ce:GAGG powders slightly decreases from 40.56 nm to 38.66 nm with increasing the calcination temperature from 900 °C to 1200 °C. However, when the calcination temperature increases to 1400 °C, the mean size of the powders increases to 151.90 nm. The large size of Ce:GAGG powders is attributed to the fusion of sintering necks that is originated from high drive energy when calcination temperature increases to 1400 °C.

2.5   Emission and excitation spectra of GAGG powders

Fig.6a and Fig.6b show photoluminescence and radioluminescence spectra of the Ce:GAGG powders co-doped with different Zn^{2+} contents under Xe lamp excitation and X-ray excitation at room temperature, respectively. All samples have similar Ce^{3+} 5d-4f emission band between 450 nm and 700 nm. It can be observed that the emission spectra show different intensities with increasing the Zn^{2+} content. As the Zn^{2+}-doped amount increases to 0.4 mol%, the sample exhibits the strongest intensity at 530 nm. From excitation spectra in Fig.6c, we can successfully figure out two excitation peaks in the ultraviolet region centered at 350 nm and blue region centered at 470 nm. Fig.6d shows a simple schematic diagram of energy transition of Ce^{3+} ions 5d→4f level.

Obviously, Zn^{2+} content has an effect on scintillation properties of Ce:GAGG powders. The main reason for this effect is that Zn^{2+} co-doping prevents the antisite defect Gd_{Ga}, in order to suppress energy loss[27]. As we
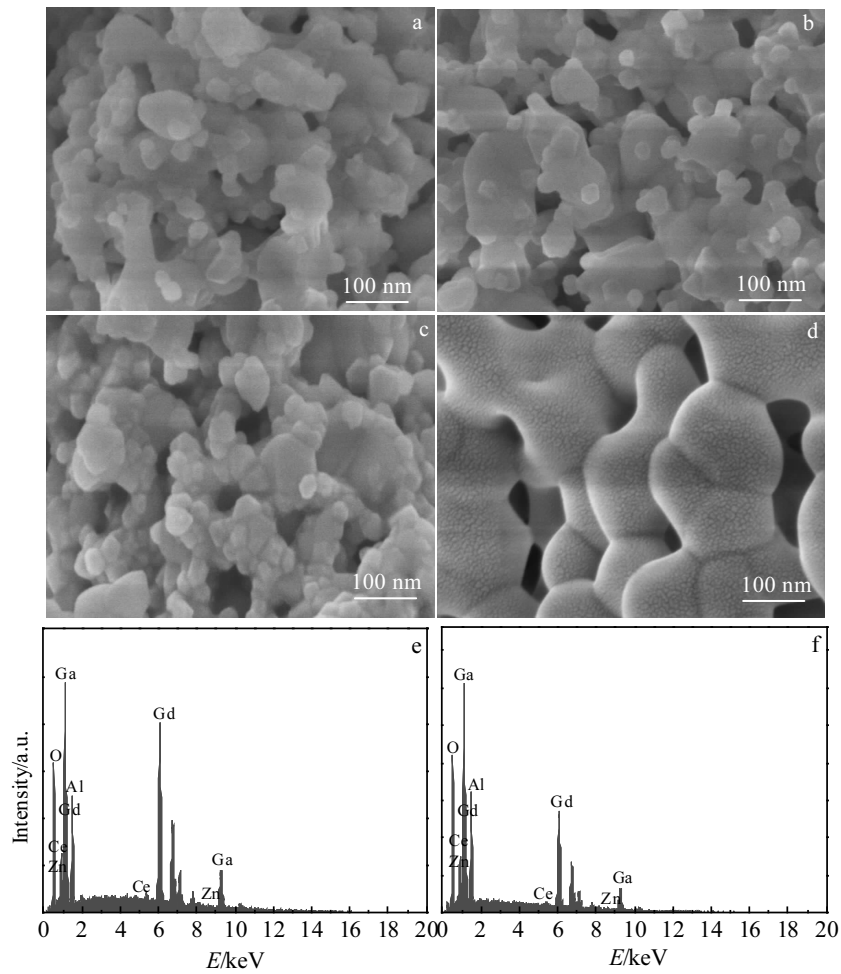
Fig.4   SEM morphologies of Ce:GAGG powders calcined at different temperatures: (a) 900 °C, (b) 1000 °C, (c) 1200 °C, (d) 1400 °C; EDS spectra of Ce:GAGG powder co-doped with 0.4 mol% Zn^{2+} (e, f)
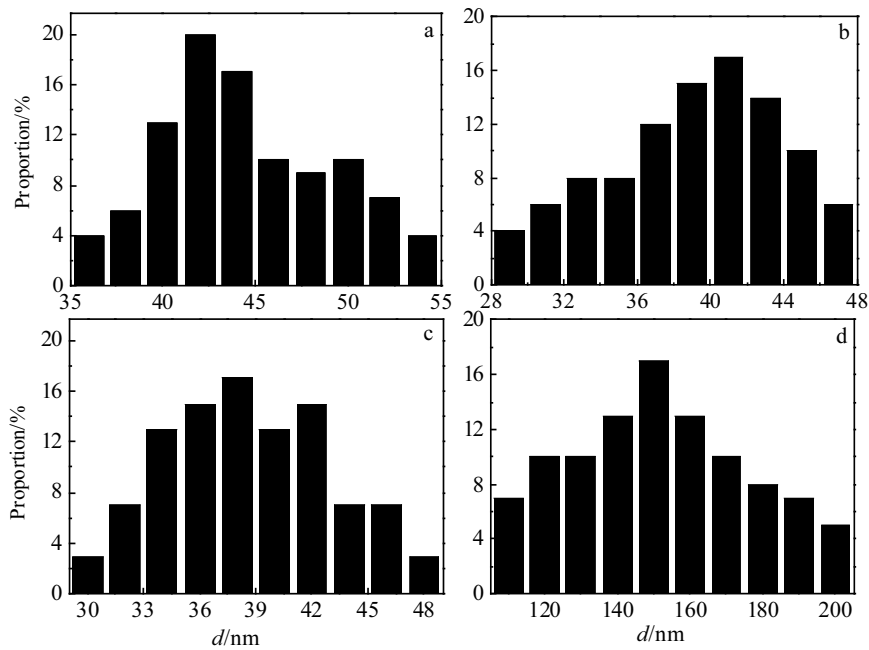
Fig.5   Particle diameter (*d*) histogram of Ce:GAGG powders calcined at different temperatures: (a) 900 °C, (b) 1000°C, (c) 1200 °C, and (d) 1400 °C

Table 1   Size range and mean size of Ce:GAGG powders

Temperature/°C	Size range/nm	Mean size/nm
900	36~54	40.56
1000	29~47	39.84
1200	30~48	38.66
1400	110~200	151.90

know, $Gd_3Al_2Ga_3O_{12}$ scintillators typically have the structure of garnet. $A_3B_2C_3O_{12}$ can succinctly show the atom composition of perfect garnets, where A, B and C are cations in different symmetry sites. In the case of Ce:YAG crystals, the antisite defects Y_{Al} appear when the dodecahedral yttrium and octahedral aluminum atom exchange positions[28]. Generally, antisite lattice defects have a lower energy barrier than other intrinsic defects. At the same time, the exchange between dodecahedral yttrium and octahedral aluminum is preferable over the exchange between dodecahedral yttrium and tetrahedral aluminum[29,30]. Besides, the decreasing of the threshold of photoionization between $5d_1$ energy level of Ce^{3+} and the bottom conduction band (CB) takes place by substitution of Ga^{3+} in B and C sites[31, 32]. Analogously, it can be inferred reasonably that antisite defects are formed by the atom exchange between dodecahedral gadolinium and octahedral aluminum. The

moderate Zn^{2+} content working as electron traps with an ideal trap depth in Ce:GAGG can maintain luminescence working by prohibiting the forming of antisite defects between dodecahedral gadolinium and octahedral aluminum. In addition, interstitial oxygen deriving from aliovalention (M^{2+}) co-doping can lower the effect of antisite defects[33, 34]. Conversely, excess Zn^{2+} content with a high electron trap concentration has negative effects on luminescence properties.

2.6   Fluorescence lifetime of GAGG powders

The fluorescence lifetime curves of Ce:GAGG powders co-doped with different Zn^{2+} contents under Xe lamp excitation ($\lambda_{ex}=350$ nm and $\lambda_{em}=530$ nm) at room temperature are shown in Fig.7. The two exponential curve approximation are used to calculate the fluorescence lifetime (τ) by the following function: $Fit=A+B_1\exp(-t/T_1)+B_2\exp(-t/T_2)$, where Fit, *B* and *T* represent the instantaneous intensity, weight of process and lifetime of process, respectively. The fluorescence lifetime of Ce:GAGG powders co-doped with different Zn^{2+} contents from 0.0 mol% to 1.0 mol% (0.0, 0.2, 0.4, 0.6, 0.8, 1.0) are 56.46, 50.58, 56.96, 49.79, 44.10 and 43.45 ns, respectively. From Fig.7, it can be discovered that fluorescence lifetime decreases with the increase of Zn^{2+} content. Therefore, the Zn^{2+} ions in Ce:GAGG
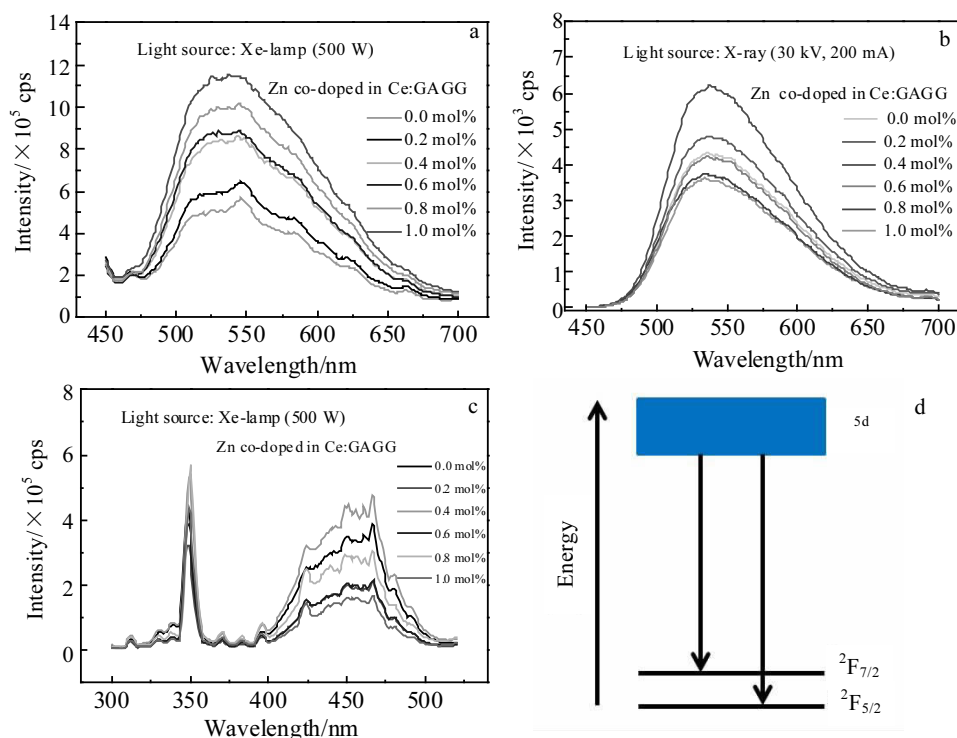
Fig.6   Photoluminescence spectra under 350 nm excitation (a), radioluminescence spectra under X-ray excitation (b), excitation spectra with 530 nm emission (c), and schematic diagram of energy transition of Ce^{3+} ions (d)
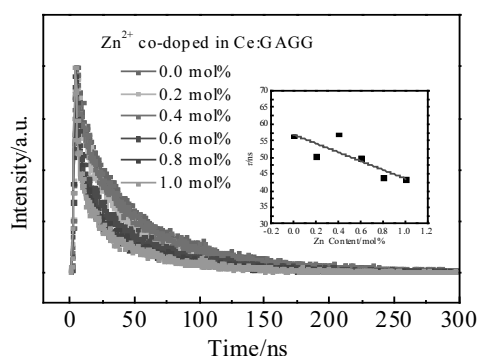
Fig.7   Fluorescence lifetime of Ce:GAGG co-doped with differ-
         ent Zn^{2+} contents under Xe lamp excitation (λ_{ex}=350 nm
         and λ_{em}=530 nm)

powders have a positive effect on the fast component
with short fluorescence lifetime.

3   Conclusions

1) A chemical co-precipitation method is introduced to
prepare Ce:GAGG powders co-doped with different Zn
contents. New phases including $GdAlO_3$ and GAGG are
generated at 883 °C. The precursors absolutely convert to
Ce:GAGG powders at 900 °C. The morphology of precur-
sors with 1 wt% PEG is more dispersive than that of pre-
cursors without PEG. The particles calcined at 1200 °C for
Ce:GAGG powders with a size of 20~60 nm become ho-
mogeneous and smooth.

2) Photoluminescence and radioluminescence spectra of
Ce:GAGG co-doped with 0.4 mol% Zn has the highest in-
tensity. On the one hand, the Zn^{2+} ion prohibits the forma-
tion of antisite defects between dodecahedral gadolinium
and octahedral aluminum. On the other hand, interstitial
oxygen deriving from aliovalention (Zn^{2+}) co-doping lowers
the effect of antisite defects.

3) Fluorescence lifetime is shortened with the increase of
Zn^{2+} content, and the Zn^{2+} ions in Ce:GAGG powders have
a positive effect on the fast component with short fluores-
cence lifetime.

References

1   Blasse G. *Chemistry of Materials*[J], 1994, 6(9):1465

2   Wisniewski D J, Boatner L A, Neal J S *et al. Proceedings of
    International Society for Optical Engineering*[J], 2007,
    6706(19): 1

3   Greskovich C, Duclos S. *Annu Rev Mater Res*[J], 2003, 27(1):
    69

4   Nikl M. *Measurement Science and Technology*[J], 2006, 17(4):
    37

5   Zych E, Brecher C, Wojtowicz A J *et al. Journal of Lumines-
    cence*[J], 1997, 75(3): 193

6   Zych E, Brecher C, Lingertat H. *Spectrochimica Acta Part A:
    Molecular and Biomolecular Spectroscopy*[J], 1998, 54(11):
    1771

7   Nikl M, Mihoková E, Mareš J A *et al. Physica Status Solidi*[J],
    2010, 181(1): 10

8   Zorenko Y, Gorbenko V, Konstankevych I *et al. Journal of
    Luminescence*[J], 2005, 114(2): 85

9   Nikl M, Yoshikawa A, Kamada K *et al. Prog Crys Growth
    Ch*[J], 2013, 59(2): 47

10 Kamada K, Yanagida T, Endo T *et al. Journal of Crystal
    Growth*[J], 2012, 352(1): 88

11 Wang Y M, Baldoni G, Rhodes W H *et al. SPIE Optical En-
    gineering+Applications*[J], 2012, 8507(17): 1

12 Chen X, Qin H, Zhang Y *et al. Journal of the American Ce-
    ramic Society*[J], 2015, 98(8): 2352

13 Kanai T, Satoh M, Miura I. *International Journal of Applied
    Ceramic Technology* [J], 2013, 10(S1): 1

14 Chewpraditkul W, Panek D, Bruza P *et al. Journal of Applied
    Physics*[J], 2014, 116(8): 707

15 Chen X, Qin H, Zhang Y *et al. Journal of the European Ce-
    ramic Society*[J], 2017, 37(13): 4109

16 Koschan M, Yang K, Zhuravleva M *et al. Journal of Crystal
    Growth*[J], 2012, 352(1): 133

17 Lin M. *Thesis for Master*[D]. Beijing: Beijing University of
    Chemical Technology, 2004

18 Vrubel II, Polozkov R G, Shelykh I A *et al. Crystal Growth
    and Design*[J], 2017, 17(4): 1863

19 Fasoli M, Vedda A, Nikl M *et al. Physical Review B*[J], 2011,
    84(8): 1855

20 Lucchini M T, Buganov O, Auffray E *et al. Journal of Lumi-
    nescence*[J], 2018, 194: 1

21 Blahuta S, Bessière A, Viana B *et al. IEEE Nuclear and
    Plasma Sciences Society*[J], 2013, 60(4): 3134

22 Wu Y T, Meng F, Li Q *et al. Physic Review Applied*[J], 2014,
    2(4): 44 009

23 Nikl M, Kamada K, Babin V *et al. Crystal Growth Design*[J],
    2014, 14(9): 4827

24 Hartshorn A J. *US Patent*, 5196180[P], 1993

25 Xie H C. *Thesis for Master*[D]. Beijing: Beijing University of
    Chemical Technology, 2013

26 Yanagida T, Kamada K, Fujimoto Y *et al. Nuclear Inst &
    Methods in Physics Research A*[J], 2011, 631(1): 54

27 Feng X Q. *Journal of Inorganic Materials*[J], 2010, 25(8):
    785

28 Muoz-García A B, Artacho E, Seijo L. *Physic Review B*[J],
    2009, 80(1): 1132

29 Kuklja M M. *Journal of Physics: Condensed Matter*[J], 2000,
    12(13): 2953

30 Milanese C, Buscaglia V, Maglia F *et al. Chemistry of
    Materials*[J], 2004, 16(7): 1232

31 Xu J, Ueda J, Kuroishi K *et al. Scripta Materialia[J]*, 2015,

102: 47

32 Ueda J, Tanabe S, Nakanishi T. *Journal of Applied Physics*[J]. 2011, 110(5): 2

33 Rozenfeld Y B, Rotman S R. *Physica Status Solidi*[J], 2010,

139(1): 249

34 Landron C, Lefloch S, Gervais M *et al. Phys Status Solidi B*[J], 2010, 196(1): 25

Zn²⁺掺杂对共沉淀法制备 Ce:Gd₃Ga₃Al₂O₁₂ 陶瓷粉体闪烁性能的影响

邱智华 [1]，张鲜辉 [2]，王帅华 [1]，吴少凡 [1]，林永红 [2]

(1. 中国科学院福建物质结构研究所 半导体光电材料及其高效转换器件协同创新中心，福建 福州 350002)

(2. 中国科学院大学，北京 100049)

摘　要：利用化学共沉淀法制备 Zn²⁺共掺的 Ce:GAGG 陶瓷粉体。研究了 Zn²⁺共掺的 Ce:GAGG 陶瓷前驱粉体的 TG/DTA 和 FTIR 曲线；分析了不同煅烧温度对 Ce:GAGG 陶瓷粉体相、形貌和颗粒度分布的影响；研究了 Zn²⁺含量对 Ce:GAGG 陶瓷粉体光致发光，辐射发光，激发光谱和荧光寿命的影响。研究表明：前驱粉体在 883 ℃的相组成为 GdAlO₃ 相和 GAGG 相；前驱粉体在煅烧温度为 900 ℃时，完全转化为 GAGG 相；当煅烧温度为 1200 ℃时，GAGG 颗粒尺寸控制在 20~60 nm，分布均匀；随着 Zn²⁺含量的变化，光致发光和辐射发光强度也相应变化，特别的，当 Zn²⁺含量为 0.4 mol%时，光致发光和辐射发光强度达到最大值；随着 Zn²⁺掺杂含量的上升，荧光寿命出现下降的趋势。因此，Zn²⁺含量对 Ce:GAGG 陶瓷粉体的辐射发光具有明显的影响，对降低荧光寿命具有积极的作用，对于提高 GAGG 闪烁材料的快速响应具有重要意义。

关键词：共沉淀法；前驱粉体；Ce:GAGG陶瓷粉体；Zn²⁺共掺杂

作者简介：邱智华，男，1990 年生，硕士，中国科学院福建物质结构研究所，福建 福州 350002，电话：0591-63179150，E-mail: qzh@fjirsm.ac.cn